DELPHI Collaboration DELPHI 2001-088 CONF 516
June 24, 2001

Search for Single Top Production at LEP via FCNC at $\sqrt{s} = 189 - 208$ GeV

Preliminary

V.Obraztsov, S.Slabospitsky and O.Yushchenko
IHEP, Protvino, Russia

S. Andringa, P. Gonçalves, A. Onofre, L. Peralta, M. Pimenta and B. Tomé
LIP-IST-FCUL, Av. Elias Garcia, 14, 1, P-1000 Lisboa, Portugal

Abstract

A search for Flavour Changing Neutral Currents was performed using the data taken by the DELPHI detector at LEP2. The data analysed were accumulated at centre-of-mass energies ranging from 189 to 208 GeV. Limits at 95% confidence level were obtained on the anomalous coupling parameters κ_γ and κ_Z. All results are preliminary.

Contributed Paper for EPS HEP 2001 (Budapest) and LP01 (Rome)

1 Introduction

Flavour Changing Neutral Currents (FCNC) are, due to the GIM mechanism, highly suppressed in the Standard Model (SM), but small contributions can appear at one-loop level due to CKM mixing [1]. On the other hand, many extended models such as supersymmetry [2] and multi-Higgs doublet models [3] predict the presence of FCNC already at tree level. Some specific models [4] give rise to detectable FCNC amplitudes.

The most prominent signature for direct observation of FCNC processes is the production of a top quark together with a light quark in the process $e^+e^- \to t\bar{c}$ [1].

The strength of the transitions $\gamma \to \mathrm{ff}'$ and $Z \to \mathrm{ff}'$ can be described in terms of the Lagrangian given in [5]:

$$\Gamma^{\gamma}_{\mu} = \kappa_{\gamma}\frac{ee_q}{\Lambda}\sigma_{\mu\nu}\left(g_1 P_l + g_2 P_r\right)q^{\nu}, \quad (1)$$

$$\Gamma^{Z}_{\mu} = \kappa_{Z}\frac{e}{\sin 2\Theta_W}\gamma_{\mu}\left(z_1 P_l + z_2 P_r\right)q^{\nu}, \quad (2)$$

where Λ is the new physics scale, e is the electron charge, e_q the top quark charge and Θ_W is the weak mixing angle. The relative contributions of the left- and right-handed components of the currents g_i and z_i obey the constraints:

$$g_1^2 + g_2^2 = 1, \quad z_1^2 + z_2^2 = 1.$$

To estimate the parameters κ_γ and κ_Z one can consider the situation in which the interference term that depends on g_i and z_i becomes negative and decreases the cross-section of the process $e^+e^- \to t\bar{c}$. This corresponds to the requirement [5]:

$$g_1 z_1 + g_2 z_2 = -1.$$

This note is devoted to the search for FCNC processes with $t\bar{c}$ production. The t quark would decay predominantly into Wb, giving distinct signatures both in the leptonic and hadronic W decay modes. A nearly background-free signature is obtained for the decays $W \to l\nu$, while the branching ratio is relatively low. The hadronic W decays gives an event rate about three times higher, but the background situation is less favourable.

Numerical estimations of the expected number of events taking into account the limits on anomalous vertices recently set by the CDF collaboration [6] can be found in [5].

The data collected with the DELPHI detector [7] at $\sqrt{s} = 189 - 208$ GeV, well above the $t\bar{c}$ production threshold, were used in this analysis. The statistics accumulated at each centre-of-mass energy is given in table 1.

The background process $e^+e^- \to Z\gamma$ was generated with PYTHIA 6.125 [8]. For $\mu^+\mu^-(\gamma)$ and $\tau^+\tau^-(\gamma)$, DYMU3 [9] and KORALZ 4.2 [10] were used, respectively, while the BHWIDE generator [11] was used for Bhabha events. Simulation of four-fermion final states was performed using EXCALIBUR [12] and grc4f [13]. Two-photon interactions giving hadronic final states were generated using TWOGAM [14]. The generated signal and background events were passed through the detailed simulation of the DELPHI detector and then processed with the same reconstruction and analysis programs as the real data.

[1] Throughout this paper the notation $t\bar{c}$ stands for for $t\bar{c}+t\bar{u}$ and includes the charge conjugate contribution as well.

$\sqrt{s}$ (GeV)	189	192	196	200	202	205	207
Luminosity (pb $^{-1}$)	151.8	25.9	76.4	83.4	40.1	78.8	84.3

Table 1: Luminosity collected by DELPHI for each centre-of-mass energy. For $\sqrt{s} >$ 202 GeV the data were collected during the year 2000 and split into two energy bins for the semileptonic analysis and for the hadronic channel both bins were considered together.

2 Hadronic Channel

In this analysis the events were preselected according to the standard hadronic selections described in [15]. An additional cut was applied, suppressing events with leptons with momenta above 20 GeV/c identified as *standard* electrons or *loose* muons according to the DELPHI lepton identification algorithms described in [7].

The LUCLUS algorithm with $D_{join} = 6.5$ was then applied to perform the event clusterization into jets. Events with 4, 5, or 6 jets were selected and forced into a 4-jet topology. Each of the three most energetic jets should contain at least one charged track. The preselection stage was completed by requiring the visible energy of the event to be greater than 130 GeV. The energies and momenta of jets were then rescaled by applying a four-constraint fit.

The jet assignment to quarks is not straightforward as the kinematics of the event strongly varies with the energy. Four different methods of jet assignment can be considered:

1. the jet with highest b-tag parameter [16] is the b-jet candidate and the softest jet is the c-jet candidate;

2. the most energetic jet is the b-jet candidate and the softest jet is the c-jet candidate;

3. the jet with highest b-tag parameter is the b-jet candidate and 2 jets are assigned to the W according to the probability of the kinematic fit;

4. the most energetic jet is the b-jet candidate and 2 jets are assigned to the W according to the probability of the kinematic fit.

All the above methods were studied and the highest efficiency for the signal and strongest background suppression was obtained with the first method. Method (2), well suited at the kinematic threshold of single top production, is less efficient at the highest LEP energies because the energy of the c jet becomes compatible with the energies of the jets coming from the hadronic decay of the W.

The further analysis was based on a likelihood ratio method. Eight variables were chosen to construct the likelihood:

- the event thrust value;
- the event sphericity;
- the global b-tag (B_{tag}) calculated with the combined algorithm [16];

- the energy of the jet assigned as b-jet (E_b);
- the energy of the most energetic jet in the event ($E_{\rm max}$);
- the ratio of the energies of the softest and most energetic jets ($E_{\rm min}/E_{\rm max}$);
- the invariant mass of the two jets assigned as originating from the W decay (M_W);
- the momentum of the reconstructed W (P_W).

Examples of relevant distributions are shown in figures 1 and 2.

Probability density functions were estimated for the individual signal (P_i^{signal}) and background (P_i^{back}) distributions and the discriminating variable:

$$W = log(\mathcal{L}_{\mathcal{S}}/\mathcal{L}_{\mathcal{B}}), \quad \text{with} \quad \mathcal{L}_{\mathcal{S}} = \left(\prod_{i=1}^{8} P_i^{\rm signal}\right) \quad \text{and} \quad \mathcal{L}_{\mathcal{B}} = \left(\prod_{i=1}^{8} P_i^{\rm back}\right)$$

was calculated for every event. Figure 3 shows the distributions for signal events, data and Monte Carlo (MC) WW events. The bottom-right plot shows the number of accepted data events as a function of the signal efficiency. The number of data events and expected background from the SM simulation passing the likelihood ratio selection are shown in table 2 for all centre-of-mass energies, together with the signal efficiencies. A good agreement with the Standard Model expectations is observed.

$\sqrt{s}$ (GeV)	Eff. (%)	Expected	Observed
189	16.4 ± 0.5	29.75 ± 1.23	29
192	17.4 ± 0.5	3.18 ± 0.38	3
196	16.3 ± 0.5	10.93 ± 0.48	14
200	16.5 ± 0.5	11.55 ± 0.48	12
202	16.4 ± 0.5	5.60 ± 0.27	5
205-207	16.4 ± 0.5	26.24 ± 0.84	21

Table 2: Signal efficiencies and numbers of observed and expected events for the hadronic channel for the different centre-of-mass energies.

3 Semileptonic Channel

In the semileptonic channel the final state corresponding to the single top production is characterized by two jets and at least one well isolated lepton from the W leptonic decay.

At the preselection level, events with a visible energy greater than 20% of the centre-of-mass energy and at least 7 charged tracks were selected and classified according to the number of isolated leptons.

The reconstruction of isolated leptons consisted on constructing double cones centered on the direction of the charged particles and requiring the energy in the inner one (half opening angle of 5°) to be above 4 GeV. The energy contained between the inner and the outer cone was required to be small, to ensure isolation. Both the opening angle of the

outer cone and the energy contained between the two cones were allowed to vary according to the energy and classification of the reconstructed particle. Lepton identification was based on the standard DELPHI algorithms described in [7, 17].

Events with at least one charged lepton were selected, and all the other particles were forced into two jets by using the Durham jet algorithm [18]. It was additionally required that the momentum of the most energetic lepton (jet) was greater than 10 GeV/c (5 GeV/c) and the polar angle of the lepton and of both jets was in the region $20^\circ \leq \theta_{lep} \leq 160^\circ$ and $10^\circ \leq \theta_{j1,j2} \leq 170^\circ$, respectively. The missing energy had to be above 25 GeV and the missing momentum polar angle was also required to be above 10° and below 170°. The combined b-tag parameter [16] was required to be greater than -2.

The energies and momenta of the jets and of the lepton were rescaled by a four-constraint fit. Events with χ^2 lower than 7 were accepted, provided the mass of the two jets and the mass reconstructed with the missing momentum and the isolated lepton were both below 120 GeV/c^2. The most energetic jet was assigned to the b quark and the second jet to the c quark. The top mass was reconstructed as the invariant mass of the b jet, the isolated lepton and the missing momentum.

Figures 4 and 5 show some relevant distributions for data and MC, after the preselection level and for $\sqrt{s} \simeq 205$ GeV. The number of events selected at this stage of the analysis for each centre-of-mass energy is given in table 3.

After the pre-selection level, a discriminating variable was constructed using the following variables:

- momentum of the less energetic jet;
- combined event b-tag variable;
- reconstructed mass of the two jets;
- reconstructed top mass;
- angle between the two jets;
- lepton-neutrino invariant mass;
- $q_l \cdot \cos\theta_l$, where q_l is the charge and θ_l is the polar angle of the lepton;
- $q_{j1} \cdot \cos\theta_{j1}$, where $q_{j1} = -q_l$ and θ_{j1} is the polar angle of the most energetic jet;
- $p_{j1} \cdot [\sqrt{s} - p_{j1}(1 - \cos\theta_{j1\,j2})]$, where p_{j1} is the momentum of the most energetic jet and $\theta_{j1\,j2}$ is the angle between the two jets.

Correlations between these variables were studied and no visible effect on the discriminating variable was seen.

For each event a signal likelihood ($\mathcal{L}_\mathcal{S}$) and background likelihood ($\mathcal{L}_\mathcal{B}$) were computed and the discriminating variable was defined as $\log(\mathcal{L}_\mathcal{S}/\mathcal{L}_\mathcal{B})$. Figure 6 represents the discriminating variable distribution and the number of events which are accepted as a function of the discriminating variable cut for a centre of mass energy of $\simeq 205$ GeV. There is a general good agreement between the data and the SM predictions.

Table 3 shows the number of events which pass a specific cut on the discriminating variable (dependent on the centre of mass energy) for the different centre-of-mass energies. The efficiencies convoluted with the W leptonic branching ratio are also shown.

$\sqrt{s}$ (GeV)	Pre-Selection		Final Selection		
	Data	Back. ± stat.	Data	Back.±stat.±syst.	$\epsilon \times \Gamma$±stat.±syst.(%)
189	409	436.8 ± 7.8	2	3.2 ± 0.9 ± 0.7	7.8 ± 0.3 ± 0.1
192	74	74.2 ± 1.3	1	1.0 ± 0.2 ± 0.1	6.9 ± 0.8 ± 0.4
196	225	223.9 ± 4.0	1	1.9 ± 0.5 ± 0.4	6.6 ± 0.9 ± 0.4
200	231	242.1 ± 4.4	2	0.9 ± 0.3 ± 0.1	5.8 ± 0.3 ± 0.3
202	100	116.7 ± 2.0	1	2.1 ± 0.3 ± 0.3	8.6 ± 0.4 ± 0.4
205	204	226.3 ± 4.6	1	2.0 ± 0.5 ± 0.4	6.2 ± 0.3 ± 0.2
207	201	235.8 ± 4.5	2	1.5 ± 0.4 ± 0.1	5.5 ± 0.3 ± 0.3

Table 3: Number of events in the semileptonic analysis at the preselection and final selection levels, for the different centre-of-mass energies. The efficiencies convoluted with the W leptonic branching ratio are also shown.

4 Limits

Limits were derived using the modified frequentist likelihood ratio method [19]. The hadronic and semileptonic channels and the different centre-of-mass energies were combined. The number of events selected in each channel and centre-of-mass energy and the corresponding signal efficiencies were given in the previous sections.

Figure 7 shows, in the (κ_γ, κ_Z) plane, the 95% confidence level limit obtained by this analysis. The top FCNC decay widths were taken into account. The different filled areas correspond to different top mass values. The result obtained by the CDF collaboration [6] is also shown in the figure.

The limits in the $(\kappa_\gamma, \kappa_Z)$ plane were calculated with the $O(\alpha_S)$ QCD corrections in the standard form ($\delta_{QCD} = \alpha/\pi$).

The stability of the result was studied by allowing, in the semileptonic channel, an independent (and significant) variation on the selection criteria of the combined b-tag and missing energy variables. These studies were performed at the pre-selection level. The smoothing procedure applied to the physical distributions used to create the discriminant variable for signal and background was also studied. The effects of such variations on the final selection criteria were quoted has an aditional contribution to the statistical error (see table 3).

5 Summary

Data collected by the DELPHI detector at centre-of-mass energies ranging from 189 to 208 GeV were analysed in the search for FCNC in $t\bar{c}$ production, in the hadronic and semileptonic topologies. No deviation with respect to the SM expectations was found. Upper limits on the anomalous Lagrangian parameters κ_γ and κ_Z were derived. Due to the s-channel dominance, the LEP2 data are less sensitive to the κ_γ parameter than to κ_Z. A visible improvement is obtained on the limits derived, when compared to the ones obtained at separate energies. The comparison with the CDF result [6] is also shown

in figure 7. Results on the search for single top production were also obtained by other experiments at LEP [20] and HERA [21].

References

[1] Grzadkowski B, Gunion J.F., and Krawcyk P., *Phys. Lett.* **B268** (1991) 106;
Eilam G, Hewett J.L, and Soni A., *Phys. Rev.* **D44** (1991) 1473;
Luke M. and Savage M.J., *Phys Lett.* **B307** (1993) 387.

[2] G.M.Divitiis, R.Petronzio, and L.Silvestrini, hep-ph/9704244 (1997).

[3] D.Atwood, L.Reina, and A.Soni, SLAC-PUB-95-6927 (1995).

[4] Arbuzov B.A. and Osipov M.Yu., hep-ph/9802392 (1998).

[5] Obraztsov V.F., Slabospitsky S.R. and Yushchenko O.P., *Phys. Lett.* **B426** (1998), 393.

[6] CDF Coll., Abe F. et al., FERMILAB-Pub-97/270-E, 1997.

[7] DELPHI coll., P. Aarnio et al., Nucl. Instr. Meth. **A303** (1991) 233;
DELPHI Coll., P. Abreu et al., Nucl. Instr. Meth. **A378** (1996) 57.

[8] Sjöstrand T., *Comp. Phys. Comm.* **82** (1994) 74.

[9] Campagne J.E. and Zitoun R., *Z. Phys.* **C43** (1989) 469.

[10] Jadach S., Ward B.F.L. and Was Z., *Comp. Phys. Comm.* **79** (1994) 503.

[11] Jadach S., Placzek W. and Ward B.F.L., *Phys. Lett.* **B390** (1997) 298.

[12] Berends F.A., Pittau R., Kleiss R., *Comp. Phys. Comm.* **85** (1995) 437.

[13] Fujimoto J. et al., *Comp. Phys. Comm.* **100** (1997) 128.

[14] Nova S., Olchevski A, and Todorov T., "TWOGAM, a Monte Carlo event generator for two photon physics", DELPHI Note 90-35 PROG 152.

[15] DELPHI Coll., P.Abreu et al., *Phys. Lett.* **B393** (1997) 245.

[16] Borisov G. *Nucl. Instr. Meth.* **A417** (1998) 384. G. Borisov, C. Mariotti, DELPHI 97-16 PHYS672; DELPHI Coll., P. Abreu et al., Nucl. Inst. Meth. **A378** (1996) 57.

[17] F.Cossutti et al., "REMCLU : a package for the Reconstruction of Electromagnetic CLUsters at LEP200", DELPHI Note 2000-164 PROG 242.

[18] S. Catani et al., Phys. Lett. **B269** (1991) 432.

[19] A.L. Read, "Optimal statistical analysis of search results based on the likelihood ratio and its application to the search for the MSM Higgs boson at $\sqrt{s}$=161 and 172 GeV", DELPHI 97-158 PHYS 737.

[20] ALEPH Coll., R. Barate et a., CERN-EP-2000-102, Geneva, CERN, 21 Jul 2000, Subm. to: Phys. Lett., B; OPAL Coll. Note PN470, 23th February 2001; L3 Coll., G. Alemanni, P. Bartalini, L3 Note 2694, 2th July 2001;

[21] ZEUS Coll., M. Kuze et al. Pres. at: 15th Les Rencontres de Physique de la Vallee d'Aoste: Results and Perspective in Particle Physics, La Thuile, Valle d'Aosta, Italy, 4 - 10 Mar 2001, hep-ex/0106030 ; 6 Jun 2001. H1 Coll., Pres. 30th International Conference on High-Energy Physics ICHEP2000, Osaka, Japan, July 2000 Abstract: 961, H1prelim-00-164.

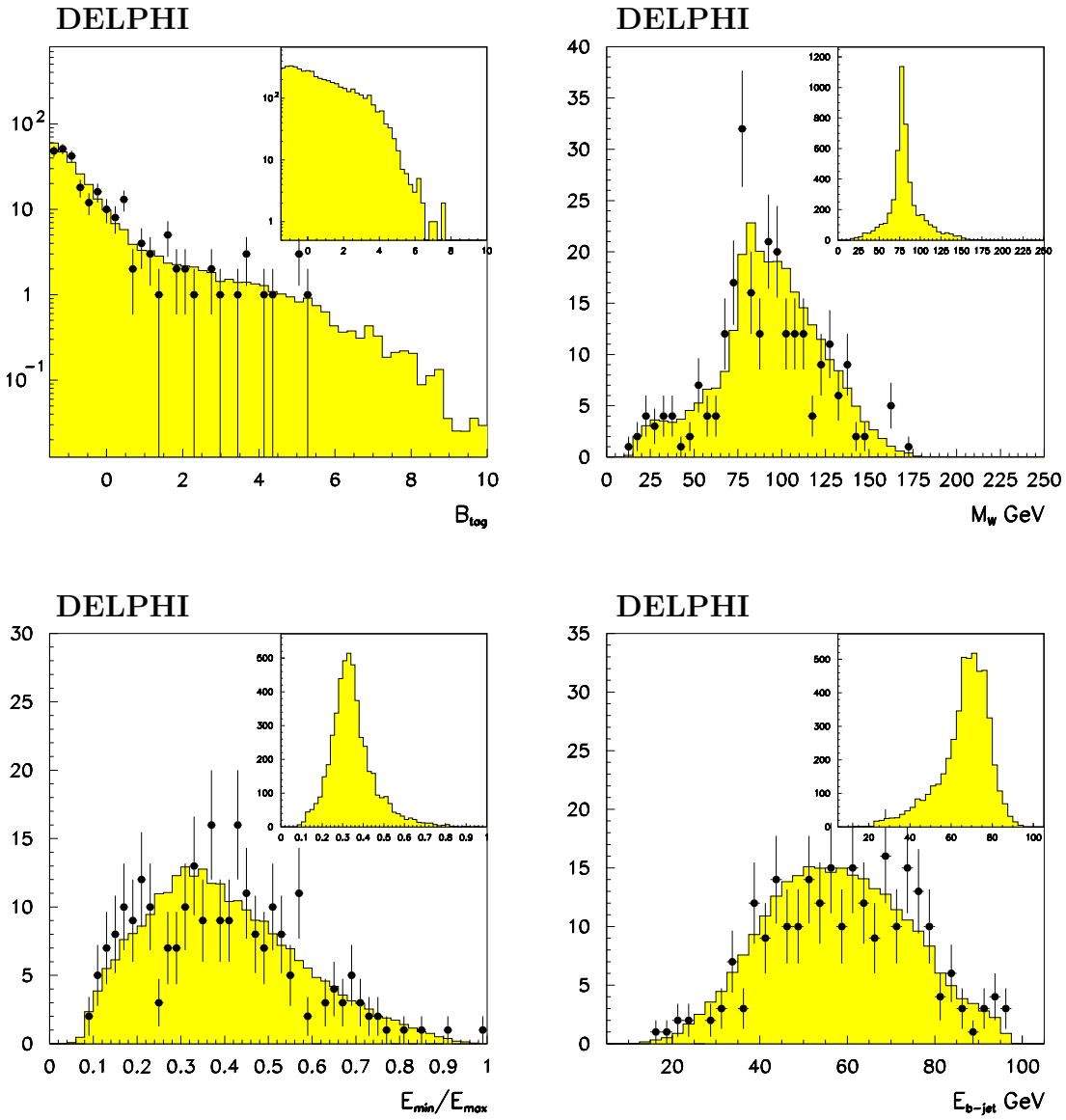

Figure 1: Distributions for the hadronic decay channel after the preselection, at $\sqrt{s} = 200$ GeV. The b-tag variable, the reconstructed W mass, the ratio between the minimal and the maximal jet energies and the energy of the most b-like jet are shown. The dots show the data and the shaded histograms show the SM simulation. The signal distribution is shown in the upper right corner.

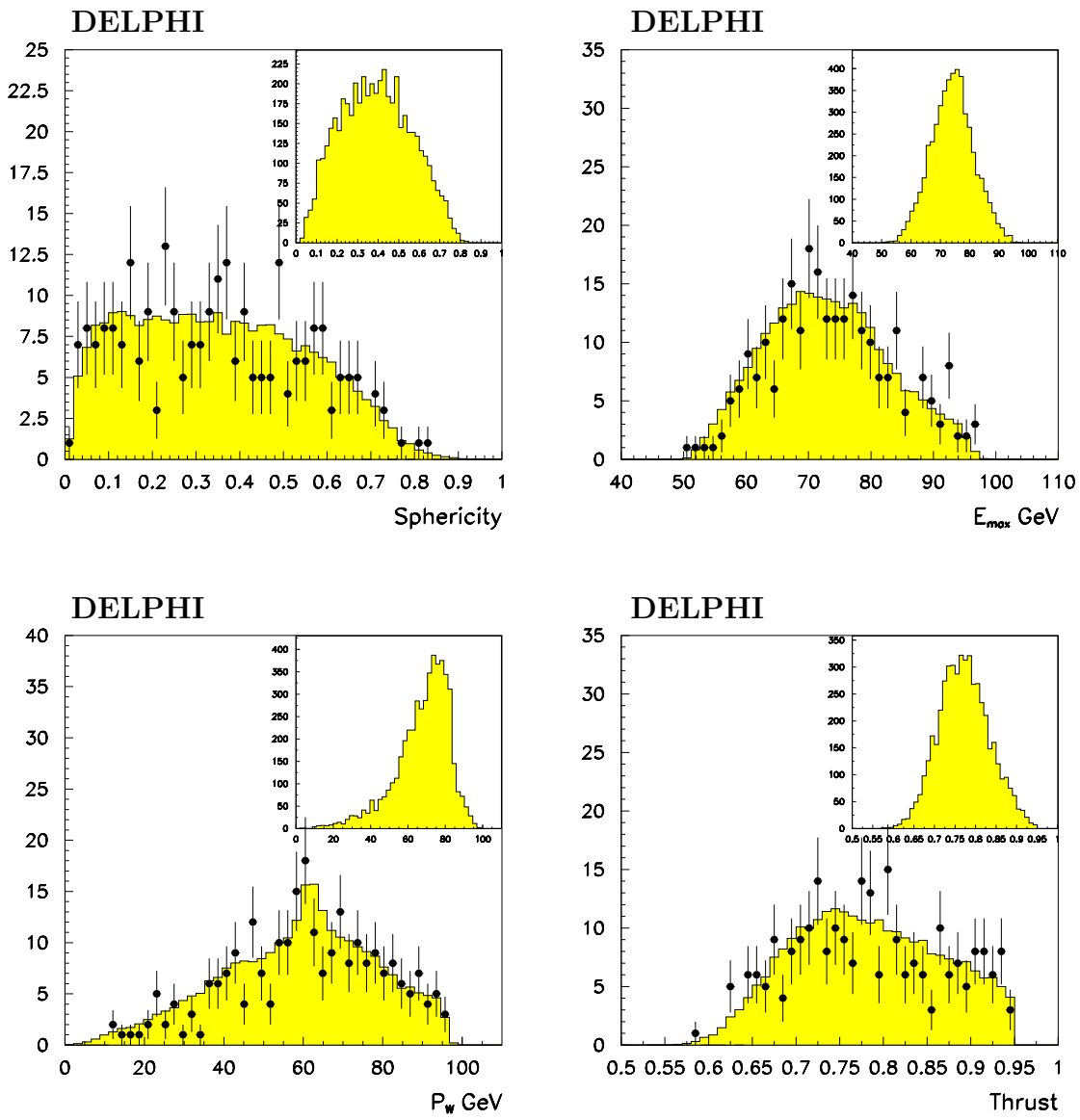

Figure 2: Distributions for the hadronic decay channel after the preselection, at $\sqrt{s} = 200$ GeV. The sphericity of the event, the energy of the most energetic jet, the reconstructed W momentum and the event thrust are shown. The dots show the data and the shaded histograms show the SM simulation. The signal distribution is shown in the upper right corner.

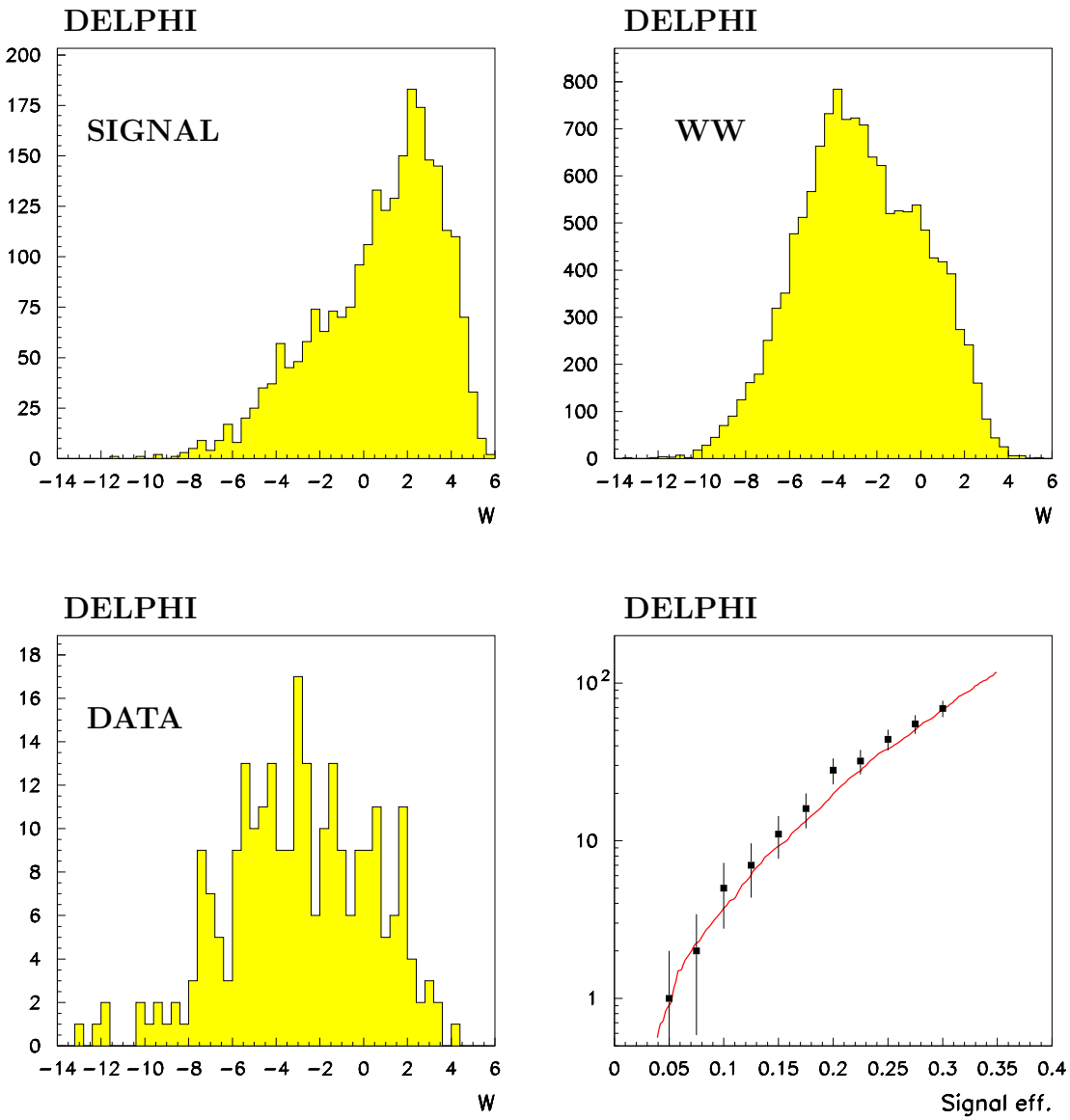

Figure 3: Distributions of the discriminating variable at $\sqrt{s} = 200$ GeV in the hadronic decay channel for signal simulation, WW background simulation and data. The bottom-right plot shows the number of accepted data events as a function of the signal efficiency. The curve shows the SM prediction.

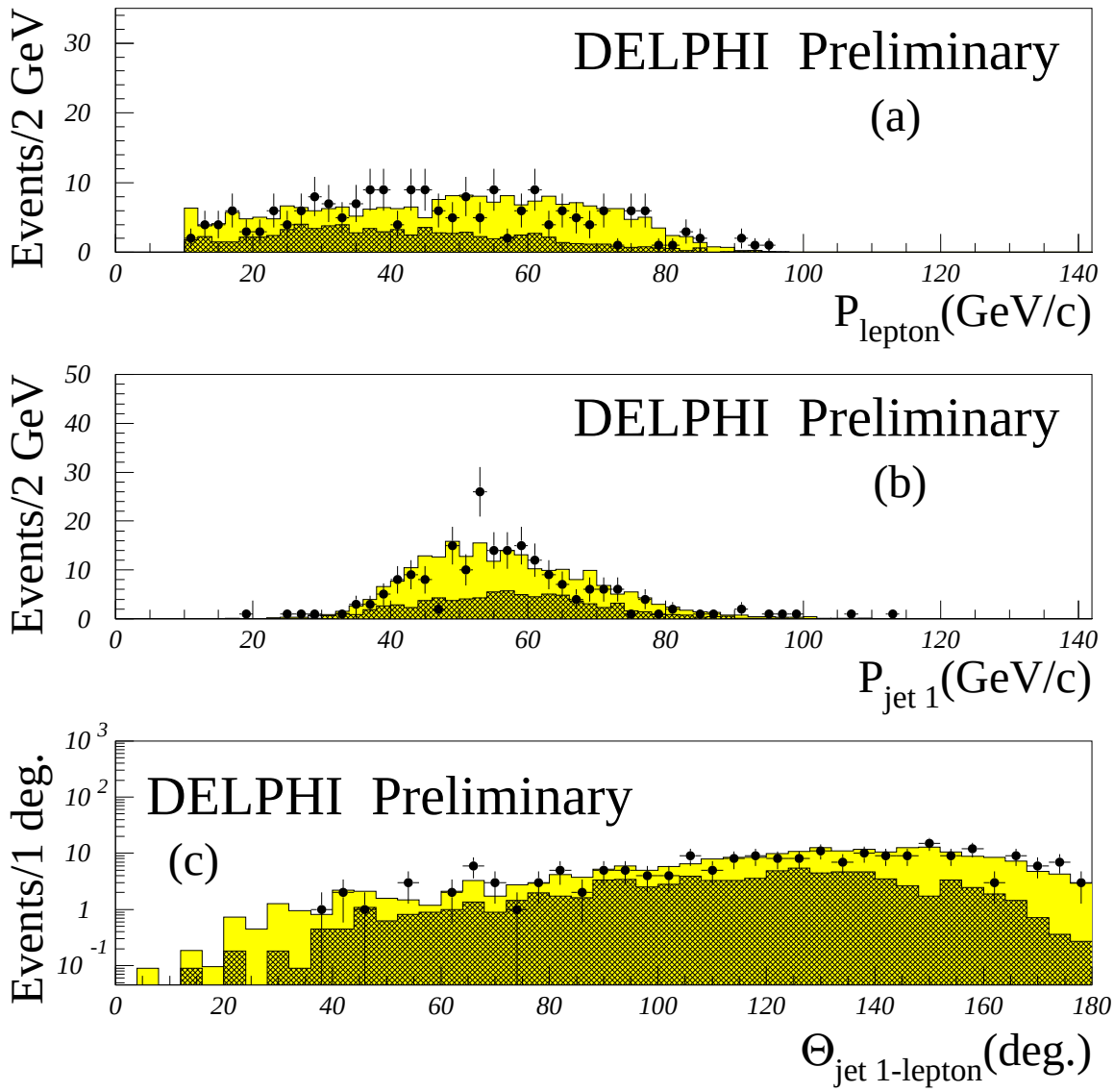

Figure 4: Distributions for the semileptonic decay channel at the preselection level for $\sqrt{s} \simeq 205$ GeV. The momentum of the most energetic lepton (a), the momentum of the most energetic jet (b) and the angle betwen them (c) are shown. The dots show the data, the shaded region the SM simulation and the dark region the expected signal behaviour.

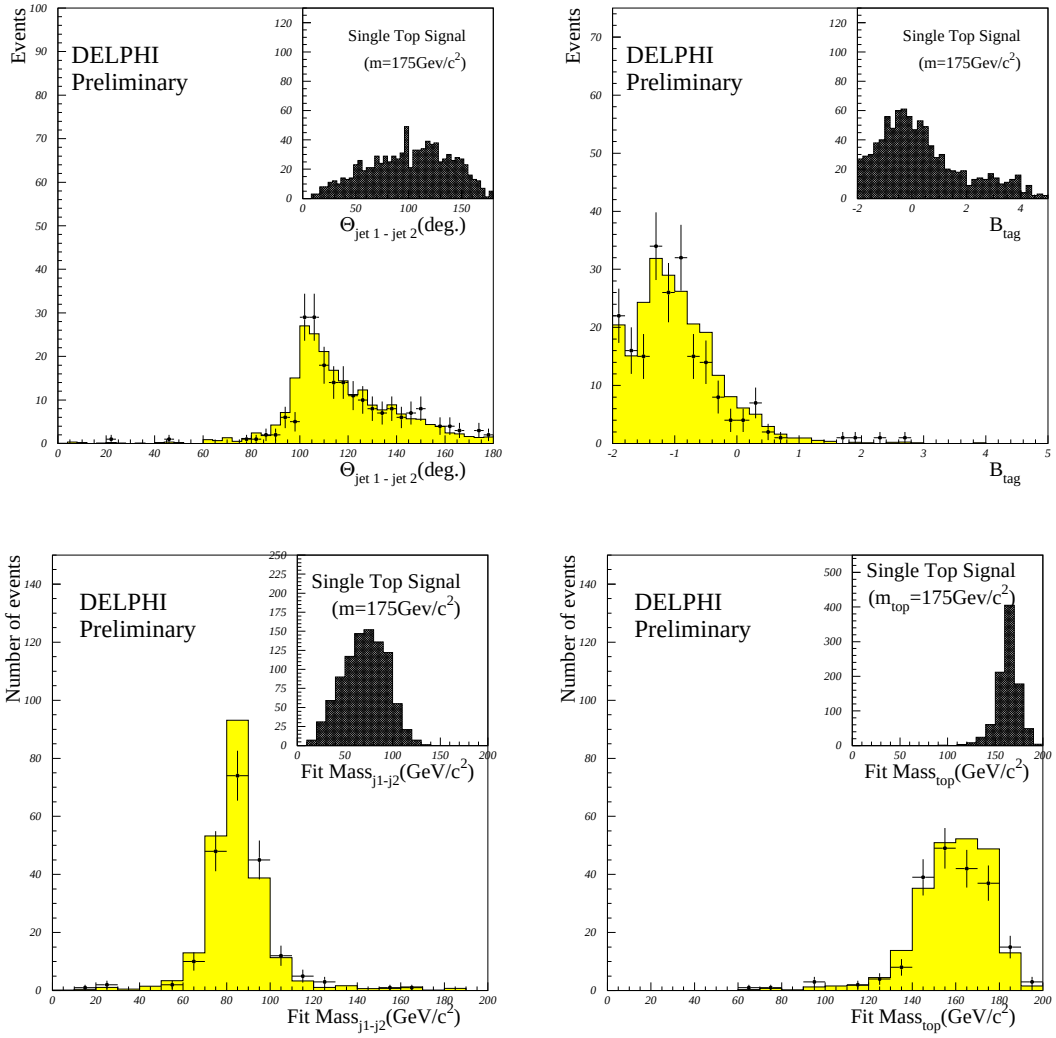

Figure 5: Distributions at the preselection level in the semileptonic decay channel, at a centre-of-mass energy of $\simeq$ 205 GeV. The angle between the two jets (top-left), the event combined b-tag variable (top-right), the two jet reconstructed mass (bottom-left) and the reconstructed top mass (bottom-right) are shown. The dots show the data and the shaded region shows the expected SM background. The top right distribution show a signal for a top with a mass of 175 GeV/c^2.

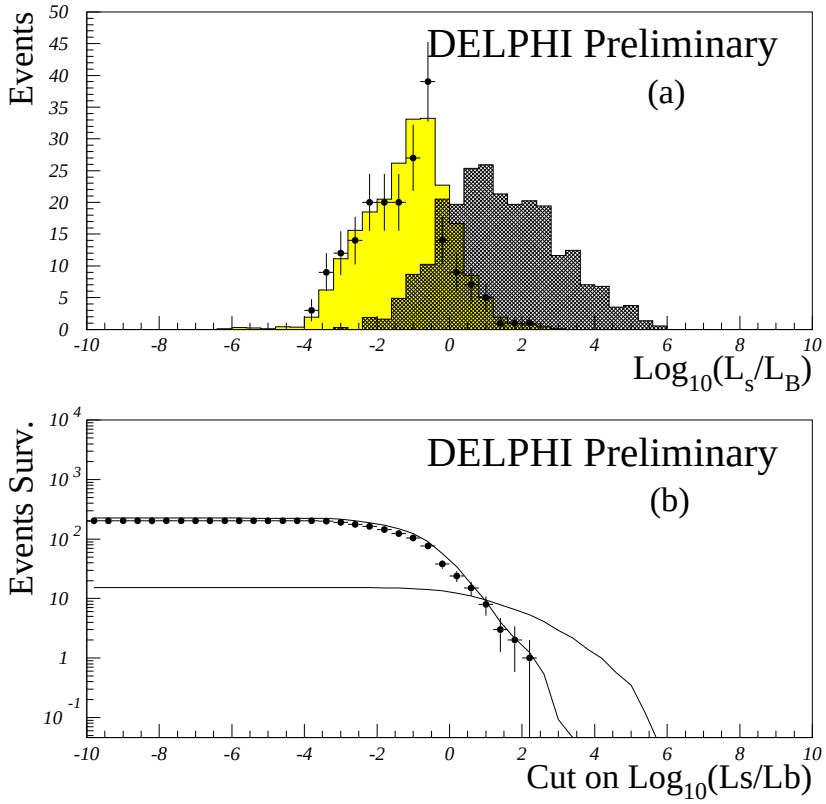

Figure 6: The discriminating variable (a) and the number of accepted events as a function of the cut on the discriminating variable (b) for a centre-of-mass energy of 205 GeV. The dots show the data, the shaded region the SM simulation and the dark region the expected signal behaviour. In (b) the line represents the signal efficiency convoluted with the W leptonic branching ratio (%) as a function of the discriminating variable cut.

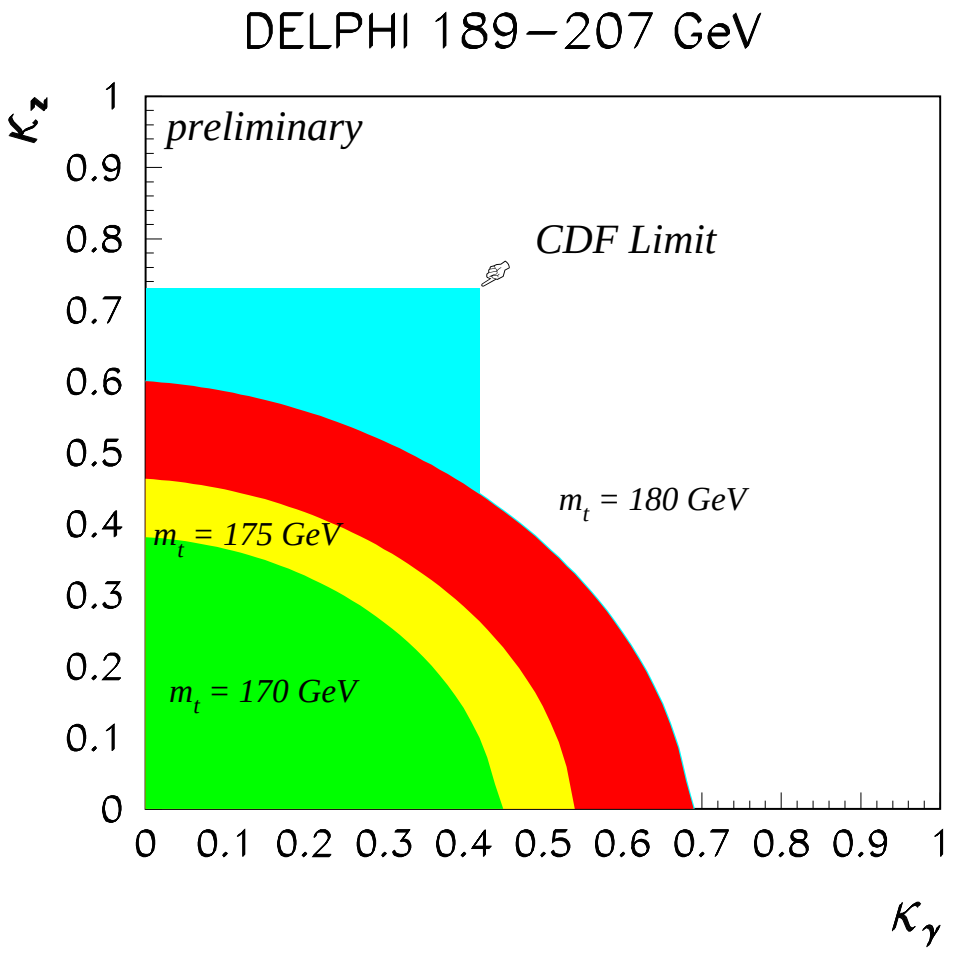

Figure 7: Limits at 95% confidence level in $\kappa_\gamma - \kappa_Z$ plane. The different areas correspond to different top quark masses.